Computer Standards & Interfaces 84 (2023) 103703

Contents lists available at ScienceDirect

Computer Standards & Interfaces

journal homepage: www.elsevier.com/locate/csi

A deep neural network approach with hyper-parameter optimization for vehicle type classification using 3-D magnetic sensor☆

Burak Kolukisa [a,*], Veli Can Yildirim [c], Cem Ayyildiz [c], Vehbi Cagri Gungor [a,b]

[a] Department of Computer Engineering, Abdullah Gül University, Kayseri, Turkey
[b] Akademi ArGe, Erciyes Teknopark, Kayseri, Turkey
[c] Department of R&D, GOHM, Muğla, Turkey

ARTICLE INFO

Keywords:
Magnetic sensors
Vehicle classification
Intelligent transportation systems

ABSTRACT

The identification of vehicle types plays a critical role in Intelligent Transportation Systems. In this study, battery-operated, easy-to-install, low-cost 3-D magnetic traffic sensors have been developed for vehicle type classification problems. In addition, a new machine learning approach based on deep neural networks (DNN) with hyper-parameter optimization using feature selection and extraction methods has been proposed for vehicle type classification. A dataset is collected from the field, and vehicles are classified into three different classes, i.e., light: motorcycles, medium: passenger cars, and heavy: buses, based on vehicle structures and sizes. The proposed system is portable, energy-efficient, and reliable. The performance results show that the proposed method, which is based on a DNN classifier, has an accuracy of 91.15%, an f-measure of 91.50%, and a battery life of up to 2 years.

1. Introduction

According to the latest published data from the International Organization of Motor Vehicle Manufacturers, the total number of produced vehicles around the world in 2019 was 92 million, and currently the world vehicle population is approximately 1.32 billion [1]. The significant increase in the number of vehicles causes various problems. In recent years, specific attention has been given to intelligent transportation systems (ITS) to promote quality of life, enhance traffic administration, and improve road maintenance planning [2]. In the ITS, the traffic monitoring systems gather data, such as the number, types, and speed of vehicles, to manage roadway systems, predict transportation needs, and improve safety.

In many countries, significant investment is being made to develop, implement, and maintain traffic monitoring systems. For effective traffic planning, it is very important to classify vehicle types correctly. Recently, researchers studied different vehicle classification systems to classify vehicle types accurately. Due to significant technical challenges, various systems have been proposed using different technologies, including accelerometers [3,4], acoustic sensors [5,6], loop detectors [7,8], LIDAR [9], piezoelectric sensors [10], vibration sensors [11,12], magnetic sensors [13–22], cameras [23], and hybrid methods [24]. In Table 1, the existing studies are compared and summarized based on different technologies.

Sensor types, hardware and parameter settings, configuration processes, operating environments, resistance to weather and noise, durability (battery life), and even maintenance and installation costs are important features and requirements for these technologies. These are extremely challenging tasks when developing vehicle classification systems. One of the most challenging tasks in these studies is the weather noise resistance, which seriously affects some sensors and consequently negatively affects the performance results [14]. For example, weather/noise resistance adversely affects the performance of certain types of sensors, such as radio, Wi-Fi, LIDAR, and cameras. Despite the high cost of camera technology, its performance is adversely affected by a change in weather conditions. It has been observed that additional studies have been carried out to reduce costs and improve performance against changes in weather conditions [25,26]. Compared to other technologies, magnetic sensors are especially preferred due to their extreme climate resistance, small size, easy set-up, and reasonable price. On the other hand, given the efficacy of the machine learning (ML) algorithms in various fields [27–31], researchers are studying to

☆ This work was supported by the Turkish Scientific and Technical Research Council (TUBITAK) 1509 program under Grant no 9180036 and Eureka NGA-ITMS project (Project ID 12668).

* Corresponding author.
E-mail addresses: burak.kolukisa@agu.edu.tr (B. Kolukisa), veli.yildirim@gohm.com.tr (V.C. Yildirim), ca@gohm.com.tr (C. Ayyildiz), cagri.gungor@agu.edu.tr (V.C. Gungor).

https://doi.org/10.1016/j.csi.2022.103703
Received 24 November 2021; Received in revised form 7 October 2022; Accepted 16 October 2022
Available online 21 October 2022

Table 1
A summary of research using different technologies for vehicle type classification.

Study	Technology	Year	SS	ACC (%)	Cost	EE	Vehicle types
[3]	Accelerometer	2013	226	99.0	NA	NA	2, 3, 4, 5, 6 axle vehicles
[4]	Accelerometer	2014	142	89.0	NA	NA	Cars, cars with trailers, trucks, truck with trailers
[5]	Acoustic	2014	160	73.42	NA	NA	Light vehicles, medium vehicles, heavy vehicles
[6]	Acoustic	2020	106	71.69	NA	NA	Cars, SUVs, trucks
[24]	Hybrid	2009	50	90.0	NA	NA	Light vehicles, medium vehicles, heavy vehicles
[7]	Loop detectors	2010	1.330	94.21	NA	NA	Class 1 (cars, jeeps), class 2 (minibusses, vans), class 3 (pickups, trucks), class 4 (buses), class 5 (motorcycles)
[8]	Loop detectors	2019	21.600	91.0	NA	NA	Car with trailers, heavy goods vehicles, buses, cars, HGV with trailers, tractor with trailers, motorcycles, large goods vehicles (LGV), LGV with trailers
[10]	Piezoelectric	2014	872	86.90	NA	NA	The 13 classes of FHWA
[11]	Vibration	2014	354	80.22	NA	NA	Light vehicles, heavy vehicles
[12]	Vibration	2018	415	89.41	NA	NA	Passenger vehicles, 2 axle bus, 2, 3, 4 axle trucks, 4, 5, 6 axle trailers
[13]	Magnetic	2013	5.837	88.0	NA	NA	Cars, vans, trucks
[14]	Magnetic	2014	188	83.0	$50	NA	Class 1 (sedans), class 2 (SUVs, pickups, vans), class 3 (buses, 2-3 axle trucks), class 4 (A. buses, 4-5-6 axle trucks)
[15]	Magnetic	2015	253	93.66	NA	NA	Motorcycles, two-boxes, salons, SUVs, buses
[16]	Magnetic	2017	20.353	96.40	NA	NA	Passenger vehicles, SUVs, vans, buses
[17]	Magnetic	2017	12.085	97.65	$80	NA	Motorcycles, passenger vehicles, single-unit trucks, combination trucks, multi-trailer trucks
[18]	Magnetic	2018	1.442	80.55	NA	NA	Class 1 (sedans, SUVs), class 2 (vans, seven-seat cars), class 3 (light, medium trucks), class 4 (heavy trucks, semi-trailers)
[19]	Magnetic	2018	300	95.46	NA	NA	Motorcycles, hatchbacks, sedans, MPVs, buses, trucks
[20]	Magnetic	2019	732	95.40	NA	NA	Class 1 (trucks), class 2 (saloons, SUVs), class 3 (buses)
[21]	Magnetic	2019	412	94.41	NA	NA	Sedans, vans, buses, trucks, non-vehicles
[22]	Magnetic	2020	6.042	97.83	NA	NA	Motorcycles, sedans, SUVs, vans, cranes, medium trucks, and buses
PP	Magnetic	2021	376	91.15	$25	2 Years	Class 1 (motorcycles), class 2 (hatchbacks, sedans, SUVs), class 3 (trucks)

SS: Sample Size, ACC: Accuracy, EE: Energy Efficiency, NA: Not Available

classify vehicle types using 3-D magnetic sensors based on ML. Several ML methods are applied, such as back propagation neural networks (BPNN) [18,19], support vector machines (SVM) [17–20], random forests (RF) [18,20], extreme gradient boosting (XGBoost) [18], decision tree (C4.5) [17,20], k-nearest neighbor (KNN) [17,19,20], naive bayes [17], and convolutional neural networks (CNN) [22] on vehicle type classification using 3-D magnetic sensor.

In this study, a battery-operated, easy-to-install, low-cost 3-D magnetic sensor has been developed for vehicle type classification. In addition, a new method is proposed for vehicle type classification based on a deep neural network (DNN) classifier with hyper-parameter optimization using feature selection and extraction methods. In comparison to previous 3-D magnetic sensor-based studies, the proposed approach provides long battery lifetime and satisfactory accuracy. As far as we know, this study is the first to focus on DNN using hyper-parameter optimization with a 3-D magnetic sensor using feature selection and extraction methods to classify vehicle types. The proposed system is portable, energy-efficient, and reliable. Performance results show that the proposed method, which is based on a DNN classifier, has an accuracy of 91.15%, an f-measure of 91.50%, and a battery life of up to 2 years. The relevant dataset and the model are published on GitHub for any researcher who is interested [32].

This study is organized as follows: In Section 2, the specifics of the 3-D magnetic sensor node are presented. In Section 3, the proposed approach is described, and classification methods are introduced. In Section 4, the performance evaluations of the proposed approach and different classification algorithms are presented. The last section concludes the paper.

2. Magnetic sensor

The proposed system includes a 3-D magnetic sensor for magnetic field measurements, a mote to read the sensor outputs, a gateway for sending the data from the mote to the data center, and a web server for analyzing the data and displaying the findings. The capsule structure that protects the system from environmental factors is given in Fig. 1.

2.1. Sensor

The system architecture of a 3-D magnetic sensor node is shown in Fig. 2. The features of sensor nodes are shown in Table 2, and the cost of each component is also provided in Table 3. Most of the research efforts do not mention the cost of the sensor node. Only a few studies, such as [14,17], show that the costs of their proposed sensors are $50

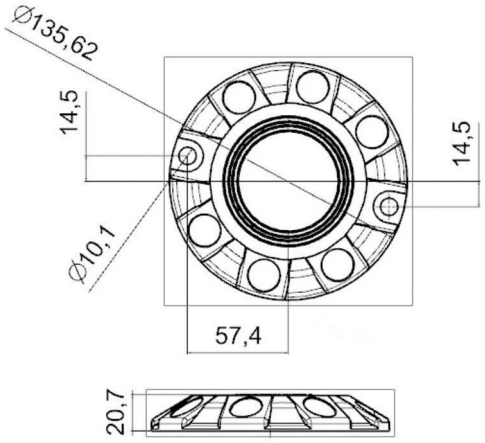

Fig. 1. Size and shape of the node.

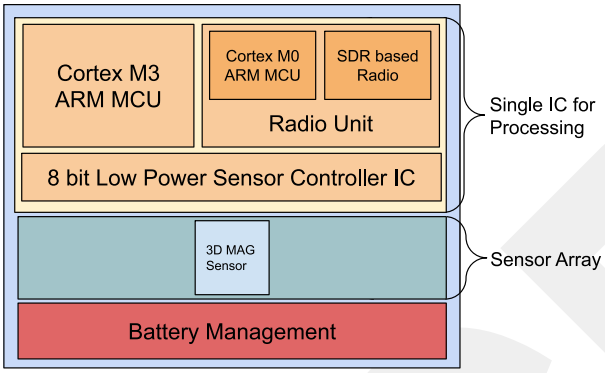

Fig. 2. System architecture.

Table 2
Sensor node features.

Feature	Description
Voltage	0.9–3.6 V
Max. Data rate	5 kbps
Tx Power	+30 dBm
RF Frequency	863–876 MHz
RF Communication distance	100 m–700 m
Operation temperature	−25 +80 °C
Mechanical robustness	10 000 kg
Waterproof IP rating	IP 67
Battery lifetime	2 years

Table 3
Cost analysis of mote.

Component part	Price
MCU (CC1312)	$7
RF Module (SE2435L)	$3
Magnetic sensor array	$5
Flash memory	$1
Antenna	$2
PCB	$7
Total	$25

and $80, respectively. The total cost of our developed sensor node is just $25, which is a substantially lower cost than those studies.

2.2. Mote

The developed mote includes a CC1312 wireless MCU having a 48-MHz Cortex-M4F microcontroller, a special radio controller based on Cortex-M0, an ultralow power 8-bit sensor controller IC, 80 kB of SRAM, UART, I2C, and SPI [33]. Communication with the gateway is ensured by the CC1312 wireless MCU operating at 868 MHz band adopting the low-rate wireless personal area network (LR-WPAN), which is an IEEE 802.15.4 communication protocol. The RF front-end module is adopted to increase the RF power output [34]. The developed embedded software on the mote is used for calibration of the sensors, reading the sensor measurements in real-time, processing and storing the collected data temporarily, and finally forwarding the stored data to the gateway. The picture of the sensor and the mote is provided with the components labeled in Fig. 3.

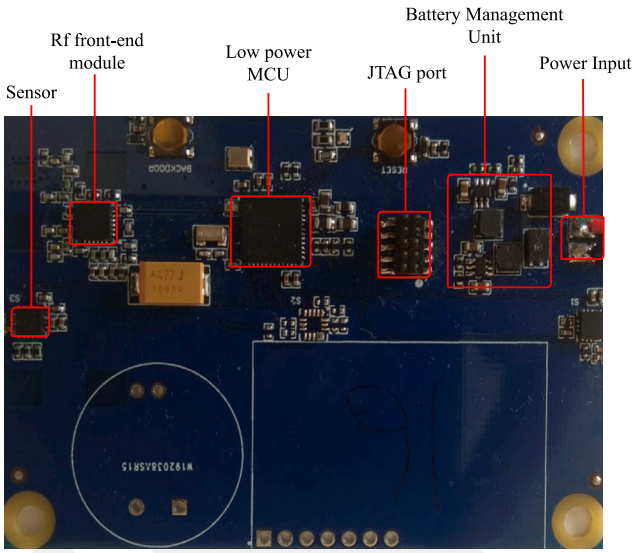

Fig. 3. The sensor and the mote.

Table 4
Gateway features.

Feature	Description
Voltage	5 V
Tx Power	+30 dBm
RF Frequency	863–876 MHz
RF Communication distance	100 m–700 m
Operation temperature	−25 +80 °C
Max. Number of connected nodes	100

2.3. Gateway

The gateway contains the same mote hardware attached to a Raspberry Pi [35]. The Linux OS runs on Raspberry Pi and relays the data collected from sensor motes to the data center. For the mote connection, the same transceiver model is used as the motes. The gateway properties are provided in Table 4.

2.4. Backend

A cloud-based backend system has been developed to categorize and save data for offline use. The camera and magnetic sensor are synchronized, which makes it easy for the user to select the time frame for trimming and classifying vehicle types in videos. A NoSQL database is used to store datasets for long-term storage.

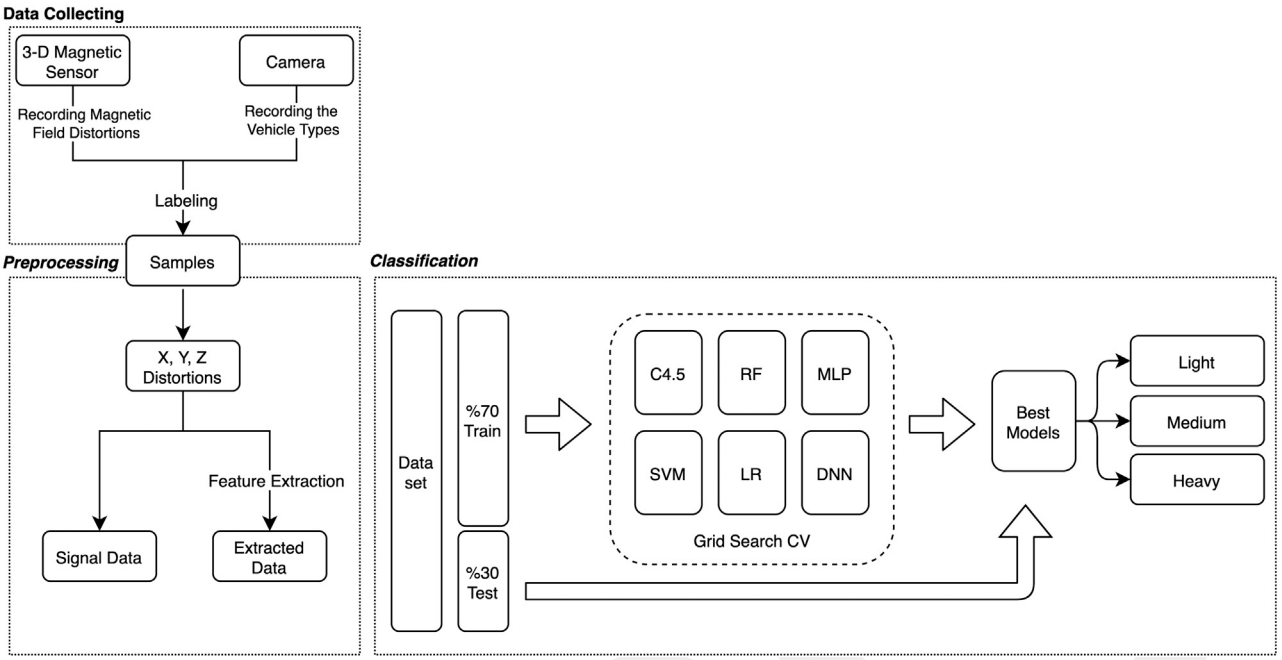

Fig. 4. Flowchart of the classification process.

2.5. Battery lifetime

Two different measurement methods are used to obtain the magnetic signature of the vehicle. The first of these methods is the time-dependent measurement method, which is continuously based on receiving data from sensors at certain time intervals. The primary advantage of this method is energy consumption. However, there is a possibility that the sensor cannot detect significant magnetic field changes, and this increases the error rate in the magnetic signature.

The second method, called vector magnitude dependent measurement, is the method that takes samples according to certain magnetic field changes (e.g., every 10 microteslas). This method's primary benefit is that, since all magnetic field changes are captured, the sample amount that can be processed is larger, and a more accurate signature can be obtained. However, adding timestamp information increases the size of the data to be transmitted in a narrow band. Accordingly, battery consumption increases significantly.

In light of this information, while the project was being implemented, the second method was used to detect magnetic changes during the vehicle's entry and exit from the sensor. The first method was used to sample the vehicle's movement on the sensor by time-based. Power consumption is optimized in this way.

While the vehicle passes over a 3-D magnetic sensor node, the magnetic sensor node wakes up, records the vehicle's measurements, transmits them to the gateway, and sleeps again. The sampling frequency of the sensor is determined as 400 Hz, which is the maximum frequency, in order to obtain better signal data and detect the vehicle's passing with minimum time loss. If the sampling frequency is lowered, the current consumption of the sensor will decrease, which increases the battery life of the sensor node. On the other hand, it will cause a decrease in the data quality and adversely affect the performance results of vehicle classification.

The sensor node was mounted on a single-lane road. A total of 50 different vehicles' magnetic distortions were measured, and the threshold (T) and references of X, Y, and Z were determined; the equation is shown in (1). For the new vehicles, magnetic distortions are shown as X_o, Y_o, and Z_o, and the vehicles' reference magnetic distortions are X_r, Y_r, and Z_r. If the equation result is greater than the T value, the vehicle's magnetic distortions start to be recorded The magnetic distortions of the 50 different vehicles were used to determine that T is equal to 110.

$$\sqrt[2]{(X_o - X_r)^2 + (Y_o - Y_r)^2 + (Z_o - Z_r)^2} > T \quad (1)$$

The sensor consumes 20 μA during the sleep period, 40 mA during the measurement period, and 425 mA during the packet transmit. In total, it draws 5420 mA in 20 ms for a vehicle. A vehicle's average power consumption is shown in Table 5.

Table 5
A vehicle's average power consumption.

Name	Average current (per ms)	Duration
Sensor measurement	40 mA	8 ms
Packet transmit (Pre-processing)	10 mA	2 ms
Packet transmit (RX)	1 A	5 ms
Packet transmit (TX)	20 mA	3 ms
Packet transmit (Post-processing)	10 mA	2 ms

3. Vehicle classification

A camera and a 3-D magnetic sensor node are used to generate the dataset. A camera takes video, while a 3-D magnetic sensor node records magnetic disturbances of the vehicles, and these processes happen concurrently. The labeling process of the magnetic disturbances was made based on the recorded video. In our previous study [36], we investigated the performance of different deep learning approaches on vehicle type classification. Different from our previous study, this paper focuses on deep neural network methods with hyper-parameter techniques using feature selection and extraction methods. Specifically, the first signal dataset (named signal data) is obtained after zero-padding is applied to the raw signal, which is obtained from the magnetic sensor node. New features are extracted from the raw signal, yielding a total of 44 features, which form our second dataset (named extracted data). Both datasets are normalized between 0 and 1. While applying the classification process, hyper-parameter optimization is also conducted. The classification process is also applied to two datasets with three different variations. (i.) employing the first dataset; (ii.) employing the second dataset; and (iii.) employing the second dataset with the

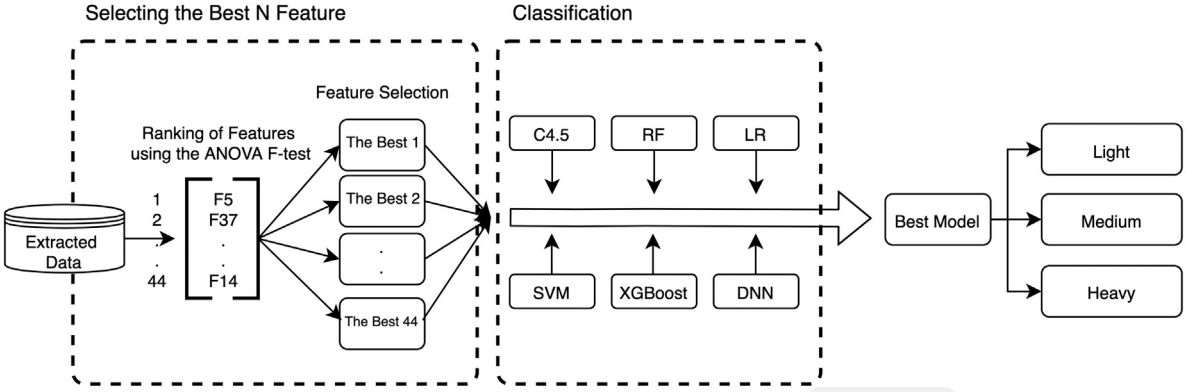

Fig. 5. Flowchart of the N best feature selections for each classifier.

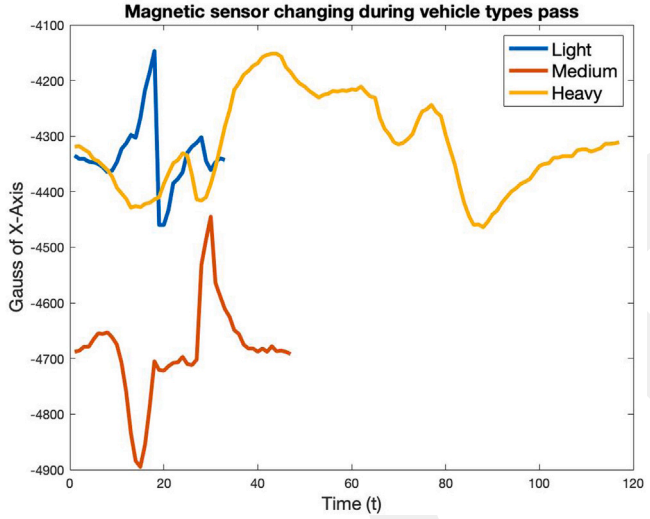

Fig. 6. Light, medium, and heavy vehicle signals, respectively.

best selected N features for each classifier. For the third variation, the second dataset is used and the ANOVA F-test method is applied to rank the features in order of importance. The appropriate Best-N features are found for each classifier via an exhaustive search. In Fig. 4, the flow chart of the classification process is shown, and in Fig. 5, finding the best N features for each classifier is shown.

3.1. Dataset

A 3-D magnetic sensor is built and mounted on a single-lane road. While the vehicle passes over the sensor, the 3-D magnetic sensor records the disturbances due to the metal materials in the vehicle. These distortions cause signal changes and differs from each other. This difference is mostly caused by the speed, physical characteristics of the vehicle, and environmental factors.

In this study, the vehicle types are divided into three categories considering the structure of the vehicle: light (L: class 1 — motorcycles), medium (M: class 2 — passenger cars), and heavy (H: class 3 — buses). In total, 376 vehicle samples are labeled (light: 46, medium: 298, and heavy: 32). The representative samples are shown in Fig. 6. T and Gauss correspond to ms and Gs, respectively. In each figure, ms varies according to the vehicle's distortion on the 3-D magnetic sensor node. The values of the X-axis are negative due to the sensor node placement on the mote.

The 3-D magnetic sensor records the raw signal data from the X, Y, and Z axes while the vehicle is passing. The vehicle's signal duration varies between 13 and 207 ms. To equalize the lengths of the samples, the signals from the samples are zero-padded according to the maximum signal duration of 207 ms. Considering the three axes for the first dataset (signal data), a total of 621 features are available for each sample. For the second dataset (extracted data), 44 features are extracted from the raw signal dataset.

3.2. Feature extraction & selection

Excess data may complicate the classification process and often lead to incorrect results. To reduce feature size and obtain better performance results, feature extraction techniques are used at this stage. As shown in Table 6, a total of 44 features are extracted. The X, Y, and Z axes shown in parentheses show that each feature is extracted separately within the three axes. For example, maximum values are extracted separately for the X, Y, and Z-axes, and a total of three features are generated. The length of the signal is the same on all three axes. Therefore, only one feature was generated.

$$\begin{cases} Average_{V_A} = \frac{\sum_1^S Mean(A)}{S} \\ Variance_{V_A} = \sqrt[2]{Mean(A) - Average_{V_A}} \end{cases} \tag{2}$$

$$\begin{cases} E_x = \frac{\sum_1^L X(k)^2}{L} \\ E_y = \frac{\sum_1^L Y(k)^2}{L} \\ E_z = \frac{\sum_1^L Z(k)^2}{L} \\ E_{all} = \frac{\sum_1^L (X(k)^2 + Y(k)^2 + Z(k)^2)}{L} \end{cases} \tag{3}$$

For the variance features, V indicates the type of vehicles: light, medium, and heavy. A indicates magnetic distortion in three axes, X, Y, and Z. S indicates the sample size of the vehicle types. First, the average signal value of each vehicle type considering the three axes is calculated. Based on the obtained average score, for each sample, in total, nine features have been extracted. The equation is as shown in (2). The equation shown in (3) calculates the energy (E_x, E_y, E_z, E_{all}) features of the X, Y, and Z, and all axes. L indicates the length of the vehicle's signal. X_k indicates the signal values of each axis in time L. For each sample, four features are generated. Energy is calculated based on the sum of the squares of the signal values divided by the length.

The performance of a model depends on the inputs, and higher quality inputs are expected to produce higher quality results. Importantly,

Table 6
Features extracted from vehicle signals.

No	Features	#
1	Maximum values (x, y, z)	3
2	Index of maximum (x, y, z)	3
3	Minimum values (x, y, z)	3
4	Index of minimum (x, y, z)	3
5	Length of signal (l)	1
6	Mean of the signals (x, y, z)	3
7	Median of the signals (x, y, z)	3
8	# of local maximum (x, y, z)	3
9	# of local minimum (x, y, z)	3
10	Mean of local maximum (x, y, z)	3
11	Mean of local minimum (x, y, z)	3
12	Variance	9
13	Energy (x, y, z, all)	4
	Total	44

Table 7
Layer configuration of DNN.

Layer names	DNN models
L1	Dense (32)
L2	Batch normalization
L3	Dropout (0.1)
L4	Dense 1 (32)
L5	Batch normalization 1
L6	Dropout 2 (0.1)
L7	Dense 2 (3)

Table 8
Hyper-parameter selection of classifier used for optimization.

Method	Parameters
C4.5	min samples split : [2–10] max depth : [1–10] min samples leaf : [1–5]
RF	max depth: 10, 20, 50, 80, 100 n estimator : 100, 200, 500, 1000
LR	penalty : l1, l2, none C : logspace(−4, 4, 20) multi class : auto, ovr, multinomial solver : newton-cg, lbfgs, liblinear, sag, saga
SVM	C : 0.1, 1, 10, 100, 1000 gamma : 1, 0.1, 0.01, 0.001, 0.0001 kernel : linear, rbf, poly, sigmoid
DNN	neurons : 32, 64, 128 neurons2 : 32, 64, 128 dropout rate: 0.1, 0.3, 0.5 dropout rate2: 0.1, 0.3, 0.5 learning rate: 10e−2, 10e−3, 10e−4 batch size: 2, 4, 6, 8
XGBoost	learning rate = [0.1–1] max depth : [1–20]

the feature selection methods remove or give lower scores to redundant features that are not relevant or have no predictive power for the target variable. The main objectives of the feature selection approaches are to minimize the complexity of the model; minimize noise; prevent overfitting; speed up ML algorithms; and enhance performance outcomes. The ANOVA F-test method is used [37,38]. Among 44 features obtained by feature extraction, features are ranked according to their importance using the ANOVA F-test method. In the experiments, the best N (1 to 44 features; N starts from 1 and is incremented one by one until 44) features have been selected, and each classification algorithm is run with different selected features as shown in Fig. 5.

3.3. Classification methods

Six classification algorithms are implemented using Python [39] with the Scikit-Learn [40] and Keras [41] libraries. These are: C4.5, RF, logistic regression (LR), XGBoost, SVM, and DNN. A DNN architecture is built with three layers containing 32, 32, and 3 neurons, respectively. The first two layers have a RELU, and the last layer has a softmax activation function. Kernel initializers are set to Glorot Uniform with a particular seed to obtain reproducible results. To prevent overfitting after each layer, batch normalization and dropout rates were added. The Adam optimizer is run with the focal loss function during the training process. In addition, the focal loss is used to reduce the impact of the class imbalance problem. The batch size is 8, the number of epochs is restricted to 30, and the early-stopping mechanism is used. With the early-stopping mechanism, model training stops after five epochs if the validation accuracy does not improve and the best weights are restored. The layer configuration of the DNN is shown in Table 7.

Focal loss is a method used to solve the class imbalance problem proposed by Lin et al. [42]. Focal loss applies a modulating term to cross-entropy loss in order to concentrate learning on a small group of difficult to classify samples and de-weight easy-to-classify samples even if their number is large during training on a classification task. This might reduce the importance of simple cases during training and swiftly concentrate the model on difficult ones; it might make the model learn efficiently. Focal loss uses Eq. (4), where CE is the regular cross-entropy loss function and FL is the focal loss. Gamma focuses more on hard examples, while the alpha offset class focuses on the imbalance of instances.

$$\begin{cases} CE(p_t) = -\alpha_t log(p_t) \\ FL(p_t) = -\alpha_t (1-p_t)^{\gamma} log(p_t) \end{cases} \tag{4}$$

The datasets are divided into two parts: 70% of the dataset is for the training set, and the remaining 30% is used for the test set. In the process of model building, 5-fold cross-validation is applied to the training set. Hyper-parameters of the models are obtained on a training set and tested on a validation set. Once the best parameters have been found, the model's best parameters are retrained with the whole training set and then tested on the test set.

3.4. Hyper-parameter optimization

Parameter optimization ensures the most appropriate parameter for the classification model. Parameters must be determined in the classification methods before training a model, and the model is trained according to these parameters. For each hyper-parameter configuration, models are trained on a training set and tested on a validation set. After the parameters that produced the best performance results on the validation set are retrained with the whole training set and then tested on the test set. The hyper-parameters for the classification methods that we have used are shown in Table 8. In this study, hyper-parameter values of all classifiers were obtained by a grid search optimization algorithm with cross-validation (GS-CV), which is a common method for finding these hyper-parameters [43,44].

4. Results & discussion

4.1. Classification methods

A detailed performance evaluation of classification methods, feature extraction, and feature selection algorithms in terms of accuracy, precision, recall, and f-measure is presented. It is critical to check other performance metrics due to the fact that the vehicles' dataset contains an imbalanced class distribution. As shown in Table 9, a comparison of classifiers between the default parameter and hyper-parameter optimization was conducted under three different variations.

Firstly, each classifier is trained using the signal dataset with default parameters and using the GS-CV hyper-parameter optimization technique. In both experiments, the best performance results are obtained with the XGBoost classifier, where the accuracy is 84.84% and the f-measure is 84.88%. Secondly, each classifier is trained using

Table 9
Performance results of classification methods.

Dataset	Hyper-parameter	# of features	Method	Accuracy (%)	Precision (%)	Recall (%)	F-measure (%)
Signal	Default	621	C4.5	78.76	81.58	71.15	79.76
			RF	82.30	83.34	67.68	82.75
			LR	78.76	79.42	66.08	78.90
			SVM	83.18	83.13	62.03	82.17
			XGBoost	84.95	84.84	70.81	84.88
			DNN	78.76	79.42	66.08	78.90
Signal	GS-CV	621	C4.5	78.76	81.58	71.15	79.76
			RF	82.30	83.34	67.68	82.75
			LR	83.18	82.82	64.99	82.39
			SVM	83.18	82.82	64.99	82.39
			XGBoost	84.84	85.05	72.71	84.84
			DNN	79.64	79.94	64.55	79.78
Extracted	Default	44	C4.5	82.30	82.30	67.78	82.19
			RF	82.30	82.70	65.67	82.49
			LR	76.99	66.32	41.46	71.15
			SVM	78.76	68.18	45.16	72.95
			XGBoost	84.95	85.47	65.84	84.68
			DNN	77.87	66.71	35.91	70.34
Extracted	GS-CV	44	C4.5	84.95	84.45	69.86	84.53
			RF	82.30	82.70	65.67	82.49
			LR	89.38	89.38	77.75	89.38
			SVM	89.38	89.82	80.71	89.56
			XGBoost	87.61	87.76	72.99	87.61
			DNN	82.30	82.30	66.73	82.30
Extracted	Default	25	C4.5	84.07	85.41	74.45	84.52
		11	RF	84.95	87.25	78.73	85.75
		5	LR	78.76	68.18	45.16	72.95
		18	SVM	84.95	85.73	64.79	84.20
		15	XGBoost	86.72	87.19	69.55	86.42
		17	DNN	86.72	86.09	67.65	86.15
Extracted	GS-CV	25	C4.5	84.95	84.45	69.86	84.53
		10	RF	85.84	88.63	83.12	86.60
		27	LR	89.38	89.38	77.75	89.38
		20	SVM	90.26	91.08	84.04	90.59
		30	XGBoost	88.49	88.72	74.31	88.43
		30	DNN	91.15	91.95	84.41	91.50

the extracted dataset with default parameters. The best performance results are obtained with the XGBoost classifier, where the accuracy is 84.95% and the f-measure is 84.68%. For the extracted dataset using the GS-CV hyper-parameter optimization technique, the best results are obtained with the SVM classifier, where the accuracy is 89.38% and the f-measure is 89.56%. Lastly, in the third set of experiments, each classifier's input size, i.e., number of features, has been changed from 1 to 44. This means that each classifier is run 44 times when the default parameters are used. The best results are obtained with the XGBoost classifier using the best 15 features, where the accuracy is 86.72% and the f-measure is 86.42%. In addition, the performance results of each classifier when using different numbers of features are also shown in Table 10. It is observed from Tables 9 and 10 that each classifier's best results differ from each other. The best results are obtained using the 25, 10, 27, 20, 30, and 30 features on C4.5, RF, LR, SVM, XGBoost, and DNN, respectively. The best results are obtained with DNN using the best 30 features, where the accuracy is 91.15% and the f-measure is 91.50%. The corresponding Best 30 features are shown in Table 11. It was observed that the effects of the extracted features, such as the mean of the signal, variance, and energy, are important for a specific axis. Only the Z-axis values are used for the variance extracted features. The effects of the extracted features, such as the maximum and minimum values and indexes, the length of the signal, the number of local maximum and minimum values, and the mean of the local minimum, are essential for all axes. In the performance results, each classifier gives better performance results when feature extraction, the best N feature selection, and hyper-parameter optimization are applied. Each of the classifier's hyper-parameters is shown in Table 12.

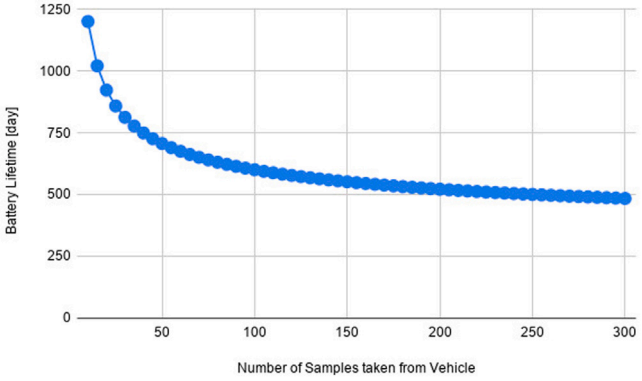

Fig. 7. Battery lifetime based on the number of samples taken from the vehicle.

4.2. Battery lifetime

In this research, we detect magnetic changes over the 3-D magnetic sensor nodes using the vector magnitude-dependent measurement method while vehicles are passing. For sampling the movement of the vehicle, the time-dependent measurement method is used. The current consumption of the sensor during the sleep state and active state (when a vehicle passes) was obtained with the help of a power analyzer named EnergyTrace. It is observed that the current consumption during a sleep state is very low, and the communication between the sensor and the gateway is the most important factor increasing the battery consumption. A data aggregation technique is used in this communication

Table 10
Performance results of the classification methods based on CV-GS and different number of features (from 5 to 40).

Methods	# of features	Accuracy (%)	Precision (%)	Recall (%)	F-measure (%)
C4.5	5	75.22	73.19	49.68	73.68
	10	80.53	81.53	67.98	80.86
	15	81.41	82.73	70.36	81.86
	20	81.41	81.72	67.41	81.39
	25	84.95	84.45	69.86	84.53
	30	83.18	83.62	71.11	83.22
	35	81.41	81.87	66.35	81.63
	40	84.95	84.45	69.86	84.53
RF	5	81.41	81.58	64.24	81.09
	10	85.84	88.63	83.12	86.60
	15	81.41	82.64	65.30	81.96
	20	83.18	83.88	68.05	83.50
	25	78.76	79.84	58.15	79.15
	30	79.64	80.64	60.54	80.05
	35	82.30	83.19	65.67	82.70
	40	81.45	82.64	65.30	81.96
LR	5	79.64	81.78	52.51	76.48
	10	84.07	84.07	71.39	84.07
	15	87.61	88.24	73.94	87.75
	20	87.61	87.80	77.00	87.59
	25	88.49	88.49	77.37	88.47
	30	89.38	89.38	77.75	89.38
	35	89.38	89.38	77.75	89.38
	40	89.38	89.38	77.75	89.38
SVM	5	75.22	63.60	34.79	68.68
	10	84.07	83.60	68.43	83.76
	15	88.49	88.91	78.33	88.69
	20	90.26	91.08	84.04	90.59
	25	86.72	87.61	75.57	87.12
	30	88.49	88.91	78.33	88.69
	35	88.49	88.49	77.37	88.47
	40	88.49	88.49	77.37	88.47
XGBoost	5	76.99	75.37	53.39	75.37
	10	80.53	80.97	64.92	80.67
	15	85.84	85.34	65.27	85.18
	20	84.95	84.12	64.89	84.30
	25	85.84	87.04	71.18	86.10
	30	88.49	88.72	74.31	88.43
	35	88.49	88.23	73.36	88.26
	40	87.61	87.28	68.97	87.02
DNN	5	77.87	65.24	35.91	70.22
	10	81.41	81.04	57.27	79.55
	15	83.18	82.05	62.14	82.49
	20	89.38	89.38	78.70	89.38
	25	87.61	87.82	77.95	87.65
	30	91.15	91.95	84.41	91.50
	35	88.49	89.63	83.29	88.86
	40	89.38	88.63	75.74	88.94

Table 11
The best 30 extracted features for the DNN classification method.

No	Features	#
1	Maximum values (x, y, z)	3
2	Index of maximum (x, y, z)	3
3	Minimum values (x, y, z)	3
4	Index of minimum (x, y, z)	3
5	Length of signal (l)	1
6	Mean of the signal (x)	1
7	Median of the signals (x, z)	2
8	# of local maximum (x, y, z)	3
9	# of local minimum (x, y, z)	3
10	Mean of local maximum (x, z)	2
11	Mean of local minimum (x, y, z)	3
12	Variance	1
13	Energy (x, all)	2
	Total	30

Table 12
Optimum hyper-parameters found using GS-CV for each classifier.

Method	Optimum hyper-parameters
C4.5	max depth = 4, min samples leaf = 1, min samples split = 4
RF	max depth = 20, n estimators = 100
LR	multi class = 'auto', penalty = 'l1', solver= 'saga', C = 4.281
SVM	C = 100, gamma = 0.1, kernel = 'rbf'
XGBoost	learning rate = 0.3, max depth = 7
DNN	neurons = 128, neurons2 = 32 dropout rate = 0.1, dropout rate = 0.3, learning rate = 10e−2, batchsize = 8

process to save power consumption and carry maximum information in minimum packet size. Furthermore, Fig. 7 gives the relationship between the lifetime of the sensor node and the number of samples obtained from the sensor node for one hundred vehicles in a day. The mean number of obtained samples from the vehicles in the dataset is 53. Considering this information and according to the current consumption characteristics of the magnetic sensor node, it has been determined that the proposed magnetic sensor node is able to run for up to 2 years without needing new batteries.

5. Conclusions

In this study, to address the vehicle type classification problem, an affordable and battery-operated 3-D magnetic sensor has been designed, and a novel approach based on a DNN classifier has been proposed. In addition, the proposed approach has been compared with six different classifiers. In comparison to previous 3-D magnetic sensor-based studies, the proposed approach provides a longer battery lifetime with satisfactory classification accuracy. As far as we know, this study is the first to focus on DNN with hyper-parameter optimization using feature selection and extraction methods on 3-D magnetic sensor nodes to classify vehicle types. Performance results show that the proposed method, which is based on a DNN classifier, has an accuracy of 91.15%, an f-measure of 91.50%, and a battery life of up to 2 years. The relevant dataset and the model are published on GitHub for any researcher who is interested [32]. Future work includes extending the proposed study with different datasets and the investigation of hybrid ML algorithms for vehicle type classification.

CRediT authorship contribution statement

Burak Kolukisa: Conception and design of study, Analysis and/or interpretation of data, Writing – original draft, Writing – review & editing. **Veli Can Yildirim:** Acquisition of data, Writing – original draft. **Cem Ayyildiz:** Conception and design of study, Acquisition of data, Analysis and/or interpretation of data. **Vehbi Cagri Gungor:** Conception and design of study, Analysis and/or interpretation of data, Writing – original draft, Writing – review & editing.

Declaration of competing interest

The authors declare that they have no known competing financial interests or personal relationships that could have appeared to influence the work reported in this paper.

Data availability

Data will be made available on request.

Acknowledgment

This research was supported by the international funding agency EUREKA with the project name "NGA-ITMS (Next Generation Autonomous Intelligent Traffic Management System)". The project is funded nationally by TUBITAK TEYDEB with Project Number: 9180036.

All authors approved the version of the manuscript to be published.

References

[1] Vehicle production statistics. oica, 2022, https://www.oica.net.

[2] F.H. Somda, H. Cormerais, J. Buisson, Intelligent transportation systems: a safe, robust and comfortable strategy for longitudinal monitoring, IET Intell. Transp. Syst. 3 (2) (2009) 188–197, http://dx.doi.org/10.1049/iet-its:20080042.

[3] W. Ma, D. Xing, A. McKee, R. Bajwa, C. Flores, B. Fuller, P. Varaiya, A wireless accelerometer-based automatic vehicle classification prototype system, IEEE Trans. Intell. Transp. Syst. 15 (1) (2013) 104–111, http://dx.doi.org/10.1109/TITS.2013.2273488.

[4] D. Obertov, B. Andrievsky, Vehicle classification using measurements from accelerometers mounted on the road surface, in: 19th International Conference on Methods and Models in Automation and Robotics (MMAR), 2014, pp. 413–417, http://dx.doi.org/10.1109/MMAR.2014.6957389.

[5] J. George, L. Mary, K.S. Riyas, Vehicle detection and classification from acoustic signal using ANN and KNN, in: International Conference on Control Communication and Computing (ICCC), 2013, pp. 436–439, http://dx.doi.org/10.1109/ICCC.2013.6731694.

[6] H. Liu, J. Ma, T. Xu, W. Yan, L. Ma, X. Zhang, Vehicle detection and classification using distributed fiber optic acoustic sensing, IEEE Trans. Veh. Technol. 69 (2) (2019) 1363–1374, http://dx.doi.org/10.1109/TVT.2019.2962334.

[7] S. Meta, M.G. Cinsdikici, Vehicle-classification algorithm based on component analysis for single-loop inductive detector, IEEE Trans. Veh. Technol. 59 (6) (2010) 2795–2805, http://dx.doi.org/10.1109/TVT.2010.2049756.

[8] M. Wasilewska, B. Golenko, Convolutional neural network based vehicle classification, in: Signal Processing Symposium (SPSympo), 2019, pp. 291–295, http://dx.doi.org/10.1109/SPS.2019.8882050.

[9] M.I. Asborno, C.G. Burris, S. Hernandez, Truck body-type classification using single-beam LiDAR sensors, Transp. Res. Rec.: J. Transp. Res. Board 2673 (1) (2019) 26–40, http://dx.doi.org/10.1177/0361198118821847.

[10] S.A. Rajab, A. Mayeli, H.H. Refai, Vehicle classification and accurate speed calculation using multi-element piezoelectric sensor, in: IEEE Intelligent Vehicles Symposium Proceedings, 2014, pp. 894–899, http://dx.doi.org/10.1109/IVS.2014.6856432.

[11] M. Stocker, M. Ronkko, M. Kolehmainen, Situational knowledge representation for traffic observed by a pavement vibration sensor network, IEEE Trans. Intell. Transp. Syst. 15 (4) (2014) 1441–1450, http://dx.doi.org/10.1109/TITS.2013.2296697.

[12] H. Zhao, D. Wu, M. Zeng, S. Zhong, A vibration-based vehicle classification system using distributed optical sensing technology, Transp. Res. Rec.: J. Transp. Res. Board 2672 (43) (2018) 12–23, http://dx.doi.org/10.1177/0361198118775840.

[13] M. Bottero, B.D. Chiara, F.P. Deflorio, Wireless sensor networks for traffic monitoring in a logistic centre, Transp. Res. C 26 (2013) 99–124, http://dx.doi.org/10.1016/j.trc.2012.06.008.

[14] S. Taghvaeeyan, R. Rajamani, Portable roadside sensors for vehicle counting, classification, and speed measurement, IEEE Trans. Intell. Transp. Syst. 15 (1) (2013) 73–83, http://dx.doi.org/10.1109/TITS.2013.2273876.

[15] B. Yang, Y. Lei, Vehicle detection and classification for low-speed congested traffic with anisotropic magnetoresistive sensor, IEEE Sens. J. 15 (2) (2014) 1132–1138, http://dx.doi.org/10.1109/JSEN.2019.2928828.

[16] F. Li, Z. Lv, Reliable vehicle type recognition based on information fusion in multiple sensor networks, Comput. Netw. 117 (2017) 76–84, http://dx.doi.org/10.1016/j.comnet.2017.02.013.

[17] W. Balid, H. Tafish, H.H. Refai, Intelligent vehicle counting and classification sensor for real-time traffic surveillance, IEEE Trans. Intell. Transp. Syst. 19 (6) (2017) 1784–1794, http://dx.doi.org/10.1109/TITS.2017.2741507.

[18] H. Dong, X. Wang, C. Zhang, R. He, L. Jia, Y. Qin, Improved robust vehicle detection and identification based on single magnetic sensor, IEEE Access 6 (2018) 5247–5255, http://dx.doi.org/10.1109/ACCESS.2018.2791446.

[19] C. Xu, Y. Wang, X. Bao, F. Li, Vehicle classification using an imbalanced dataset based on a single magnetic sensor, Sensors 18 (6) (2018) 1690, http://dx.doi.org/10.3390/s18061690.

[20] X. Zhang, H. Huang, Vehicle classification based on feature selection with anisotropic magnetoresistive sensor, IEEE Sens. J. 19 (21) (2019) 9976–9982, http://dx.doi.org/10.1109/JSEN.2019.2928828.

[21] X. Chen, X. Kong, M. Xu, K. Sandrasegaran, J. Zheng, Road vehicle detection and classification using magnetic field measurement, IEEE Access 7 (2019) 52622–52633, http://dx.doi.org/10.1109/ACCESS.2019.2908006.

[22] W. Li, Z. Liu, Y. Hui, L. Yang, R. Chen, X. Xiao, Vehicle classification and speed estimation based on a single magnetic sensor, IEEE Access 8 (2020) 126814–126824, http://dx.doi.org/10.1109/ACCESS.2020.3008483.

[23] J. Chang, L. Wang, G. Meng, S. Xiang, C. Pan, Vision-based occlusion handling and vehicle classification for traffic surveillance systems, IEEE Intell. Transp. Syst. Mag. 10 (2) (2018) 80–92s, http://dx.doi.org/10.1109/MITS.2018.2806619.

[24] E.H. Ng, S.L. Tan, J.G. Guzman, Road traffic monitoring using a wireless vehicle sensor network, in: International Symposium on Intelligent Signal Processing and Communications Systems, 2009, pp. 1–4, http://dx.doi.org/10.1109/ISPACS.2009.4806673.

[25] Y.L. Chen, B.F. Wu, H.Y. Huang, C.J. Fan, A real-time vision system for nighttime vehicle detection and traffic surveillance, IEEE Trans. Ind. Electron. 58 (5) (2010) 2030–2044, http://dx.doi.org/10.1109/TIE.2010.2055771.

[26] S.C. Huang, B.H. Chen, Automatic moving object extraction through a real-world variable-bandwidth network for traffic monitoring systems, IEEE Trans. Ind. Electron. 61(4), 20137 (2099-2112), http://dx.doi.org/10.1109/TIE.2013.2262764.

[27] R. Espinosa, D. García-Saiz, M. Zorrilla, J.J. Zubcoff, J.N. Mazón, S3mining: A model-driven engineering approach for supporting novice data miners in selecting suitable classifiers, Comput. Stand. Interfaces 65 (2019) 143–158, http://dx.doi.org/10.1016/j.csi.2019.03.004.

[28] Y. Song, Web service reliability prediction based on machine learning, Comput. Stand. Interfaces (73), 103466 (2021) http://dx.doi.org/10.1016/j.csi.2020.103466.

[29] S.H. Chin, C. Lu, P.T. Ho, Y.F. Shiao, T.J. Wu, Commodity anti-counterfeiting decision in e-commerce trade based on machine learning and internet of things, Comput. Stand. Interfaces (76) (2021) http://dx.doi.org/10.1016/j.csi.2020.103504.

[30] A.A. Afuwape, Y. Xu, J.H. Anajemba, G. Srivastava, Performance evaluation of secured network traffic classification using a machine learning approach, Comput. Stand. Interfaces (78), 103545 (2021) http://dx.doi.org/10.1016/j.csi.2021.103545.

[31] P.K. Roy, A.K. Tripathy, T.H. Weng, K.C. Li, Securing social platform from misinformation using deep learning, Comput. Stand. Interfaces (84), 103674 (2023) http://dx.doi.org/10.1016/j.csi.2022.103674.

[32] B. Kolukisa, Vehicle type classification using 3-d magnetic sensor. github, 2022, https://github.com/burakkolukisa/Vehicle-type-classification-using-3-D-magnetic-sensor.

[33] "CC1312R," CC1312R data sheet, product information and support | TI.com, 2021, http://www.ti.com/product/CC1312R.

[34] "SE2435L," skyworks, 2021, https://www.skyworksinc.com/.

[35] Raspberry Pi, "teach, learn, and make with raspberry pi," raspberry pi, 2021, https://www.raspberrypi.org.

[36] B. Kolukisa, V.C. Yildirim, B. Elmas, C. Ayyildiz, V.C. Gungor, Deep learning approaches for vehicle type classification with 3-D magnetic sensor, Comput. Netw. 217 (2022) http://dx.doi.org/10.1016/j.comnet.2022.109326.

[37] E. Girden, ANOVA: Repeated Measures, Vol. 84, Sage, 1992.

[38] M. Kuhn, K. Johnson, Feature Engineering and Selection: A Practical Approach for Predictive Models, CRC Press, 2019.

[39] G.V. Rossum, F.L. Drake, Python 3 reference manual CA: CreateSpace, 2009.

[40] F. Pedregosa, G. Varoquaux, A. Gramfort, V. Michel, B. Thirion, O. Grisel, M. Blondel, P. Prettenhofer, R. Weiss, V. Dubourg, J. Vanderplas, A. Passos, D. Cournapeau, M. Brucher, M. Perrot, E. Duchesnay, Scikit-learn: Machine learning in python, J. Mach. Learn. Res. 12 (2011) 2825–2830.

[41] F. Chollet, et al., Keras, 2015, URL https://github.com/fchollet/keras.

[42] T.Y. Lin, P. Goyal, R. Girshick, K. He, P. Dollar, Focal loss for dense object detection, in: Proceedings of the IEEE International Conference on Computer Vision (ICCV), 2017, pp. 2980–2988.

[43] T. Yu, H. Zhu, Hyper-parameter optimization: A review of algorithms and applications, 2020, http://dx.doi.org/10.48550/arXiv.2003.05689, arXiv areprint arXiv:2003.05689.

[44] L. Yao, Z. Fang, Y. Xiao, J. Hou, Z. Fu, An intelligent fault diagnosis method for lithium battery systems based on grid search support vector machine, Energy 214 (2021) 118866, http://dx.doi.org/10.1016/j.energy.2020.118866.

Burak Kolukisa received the B.S in Computer Engineering From Erciyes University, Kayseri, in 2016 and M.S. degrees in Electrical and Computer Engineering from Abdullah Gul University, Kayseri, Turkey, in 2020. Currently, he is working as a Research Assistant at the Department of Computer Engineering, Abdullah Gul University. His current research interests are Data Mining, Machine Learning, and Deep Learning. He is also a Ph.D. candidate in the Electrical and Computer Engineering program at Abdullah Gul University, Kayseri, Turkey.

Veli Can Yildirim received his B.S. degree in Control and Automation Engineering from Yildiz Technical University, Istanbul, in 2019. Currently, he is working as an Embedded Software Developer at GOHM Electronics and Embedded Intelligence Systems. His current research interests are internet of things, machine to machine communications, and wireless ad hoc and sensor networks.

Cem Ayyildiz received his B.S. degree in Electrical and Electronics Engineering from Middle East Technical University, Ankara, Turkey in 2006 and M.S. degree in Microelectronics from Bremen University of Applied Sciences, Bremen, Germany in 2008. He received his Ph.D. degree in Computer Engineering program at Bahcesehir University, Istanbul, Turkey, in 2019. Currently, he is working at GOHM, Mugla, Turkey. His current research interests are wireless and mobile communications, and Internet of things.

V. Cagri Gungor received his B.S. and M.S. degrees in Electrical and Electronics Engineering from Middle East Technical University, Ankara, Turkey, in 2001 and 2003, respectively. He received his Ph.D. degree in electrical and computer engineering from the Broadband and Wireless Networking Laboratory, Georgia Institute of Technology, Atlanta, GA, USA, in 2007. Currently, he is a Professor and Chair of Computer Engineering Department, Abdullah Gul University, Kayseri, Turkey. His current research interests are smart grid communications, machine-to-machine communications, next-generation wireless networks, wireless ad hoc and sensor networks, cognitive radio networks.